Dyes and Pigments 92 (2011) 783–788

Contents lists available at ScienceDirect

Dyes and Pigments

journal homepage: www.elsevier.com/locate/dyepig

Alkyl substituent effects on J- or H-aggregate formation of bisazomethine dyes

Kenji Kinashi [a,*], Kyun-Phyo Lee [b], Shinya Matsumoto [c], Kenji Ishida [b], Yasukiyo Ueda [b]

[a] Graduate School of Science and Technology, Department of Macromolecular Science and Engineering, Kyoto Institute of Technology, Matsugasaki, Sakyo, Kyoto 606-8585, Japan
[b] Graduate School of Engineering, Department of Chemical Science and Engineering, Kobe University, Rokko, Nada, Kobe 657-8501, Japan
[c] Graduate School of Environmental and Information Sciences, Yokohama National University, Hodogaya, Yokohama 240-8501, Japan

ARTICLE INFO

Article history:
Received 17 March 2011
Received in revised form
24 May 2011
Accepted 28 May 2011
Available online 12 June 2011

Keywords:
J-aggregates
H-aggregates
Bisazomethine dye
Functional dye
Vapor-deposited film
Optical property

ABSTRACT

Bisazomethine dyes with terminal alkyl substituents of different chain lengths (BAR: $R = 1, 2, 3, 4, 5$ and 6) were synthesized and deposited on a glass substrate to investigate the effect of the alkyl chain length on aggregate formation. Methyl- and ethyl-substituted bisazomethine dyes (BA1 and BA2) formed J-aggregates in thin films (ca. 50 nm), whereas, propyl-, butyl-, pentyl- and hexyl-substituted derivatives (BA3, BA4, BA5 and BA6) formed H-aggregates in thin films (ca. 50 nm). The aggregate formation of the BARs changed drastically between ethyl- and propyl-substituents (BA2/BA3). However, no remarkable changes were observed in the surface morphologies of BA2 and BA3 films. It is suggested that the critical determinant of aggregate formation of BAR is the molecular packing in the film, which depends on the chain length of the terminal alkyl substituent.

1. Introduction

Organic molecules can form crystals or aggregates, in which the visible absorption bands in the solid state are generally split or shifted from those of the monomeric molecules. Dye aggregates have played important roles in both fundamental science and technological applications such as optical memory, organic solar cells and organic light-emitting diodes [1–3]. In general, they are classified into two types, H- and J-aggregates [4–6]. H-aggregates adopt face-to-face stacking structures, which are characterized by a blue-shift in the absorption band. H-aggregates can effectively contribute to the photocurrent in Schottky-type photovoltaic cells where thin films are sandwiched between two different types of metal electrodes [7]. J-aggregates are characterized by a sharp absorption band (J-band) with red-shifted from that of isolated molecules and have attracted much attention for both fundamental studies and their large optical non-linearity and ultra-fast response time for nonlinear optical materials. The specific structure of the J-aggregates is a head-to-tail stacking between adjacent molecules. Intriguingly, most studies on J- or H-aggregates described them as compounds with dipole moments [8–10] and ionic features [11,12]. Thus, J-aggregate formation is irrelevant to polar and/or ionic dyes. However, Matsumoto et al. found that large and homogeneous films of J-aggregates can be formed in vapor-deposited films of *N,N′*-bis[(4-(*N,N*-diethylamino)benzylidene]diaminofumaronitrile (BA2), even though it is a non-polar (and non-ionic) dye. The packing structure of BA2 is consistent with the J-aggregate films consisting of a stable single crystal phase and a metastable crystalline phase [13]. BA2 also forms J-aggregates in vapor-deposited films depending on the film thickness (>100 nm), despite its symmetric and non-ionic molecular structure. The J-aggregate film was extremely stable such that no significant change in absorption spectra was observed even after one year at ambient conditions or after thermal treatment at 375 K for 1 h. However, despite enormous effort, sufficient understanding of the substituent effects on aggregate formations has not yet been obtained. Therefore, studies on the controlling dye aggregate formation and the formation mechanism of these aggregates in thin films are of great importance for practical applications as well as for basic research of assembled dye molecules. Recently, some interesting results have been reported by Kim et al. regarding the effect of phenyl substitution on the J-aggregation of bisazomethine dyes [14]. The absorption spectra of these dyes showed a variety of spectral changes in the visible region and some of the synthesized dyes were found to form J-aggregates in vapor-deposited films. Therefore, bisazomethine dyes are excellent candidates for the further

* Corresponding author.
E-mail address: kinashi@kit.ac.jp (K. Kinashi).

0143-7208/$ – see front matter © 2011 Elsevier Ltd. All rights reserved.
doi:10.1016/j.dyepig.2011.05.024

study of the correlation between substituent effects and the aggregation mechanism.

In this study, based on the spectroscopic evidence, the influence of the chain length of the terminal substituent on the aggregate formation was determined in order to understand the mechanism of J- and H-aggregate formation, and to guide the design of novel J- and H-aggregate organic dyes.

2. Experimental

Bisazomethine dyes (BA) with different alkyl chain lengths were synthesized. BAs with different alkyl chains are abbreviated as BAR where $R = 1, 2, 3, 4, 5$ and 6 to represent methyl-, ethyl-, propyl-, butyl-, pentyl- and hexyl-substituents, respectively. The synthetic procedure of BA dyes is shown in Scheme 1. BA1 and BA2 were synthesized from *p-N,N*-dialkylaminobenzaldehyde, BA3 and BA4 were synthesized from *N,N*-dialkylaniline, and BA5 and BA6 were synthesized from aniline. *p-N,N*-Dimethyl- and *p-N,N*-diethylaminobenzaldehyde were purchased from Nacalai Tesque, Inc. *N,N*-Dipropyl- and *N,N*-dibutylaniline were purchased from Tokyo Kasei Co., Ltd. They were used without further purification. The chemical structures of the synthesized compounds were characterized using ^{1}H NMR [Bruker Advance500, $CDCl_3$ solvent, tetramethylsilane (TMS) internal standard], FT-IR (Jasco FT/IR-600 plus) and TOF-MS (PerSeptive Biosystems Mariner) spectroscopies. Melting points (mp) were determined using a melting point apparatus (Yanaco MP-500P) with a digital thermometer. UV–visible absorption and photoluminescence (PL) spectra were recorded on JASCO V-670 and Hitachi F-2500 spectrophotometers, respectively. Measurements of absorption and PL spectra in solution were performed in a quartz cell with a path length of 1 cm. The films were prepared on a glass substrate from a quartz crucible heated by a tungsten filament in a vacuum of 10^{-4} Pa. The deposition rate was 5 nm/s and the substrate temperature was maintained at 40 °C. The film thickness was controlled at 50 nm. The morphologies of the films were characterized using an atomic force microscope (AFM, SPI-3700, Seiko Instruments).

3. Synthesis

3.1. N,N-dialkylanilines

A mixture of fresh aniline (21.5 mmol), iodoalkane (4.51 mmol), and K_2CO_3 (4.51 mmol) in EtOH (20 mL) was refluxed at 75 °C for 18 h. The suspension was filtered, and the resulting solid was washed with CH_2Cl_2. The filtered solution was extracted with water, and the organic layer was dried over anhydrous $MgSO_4$ and concentrated in vacuo. Purification by column chromatography on silica gel (eluent: $CHCl_3$) produced an oil. Products with different alkyl chains (pentyl and hexyl) were synthesized using the same procedure. Specific details for each compound are given below.

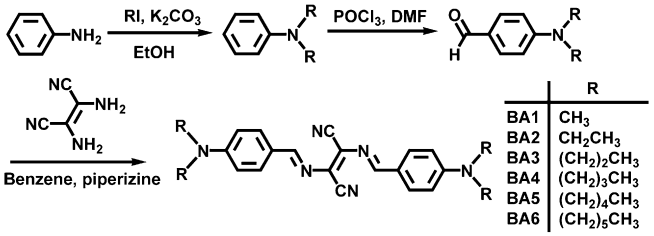

Scheme 1. Synthetic procedure for BAR.

3.1.1. N,N-dipentylaniline

70.3% yield. Product: yellow oil. FT-IR (cm^{-1}): 3986, 3647, 3412, 3093, 3061, 3024, 2958, 2873, 2735, 2649, 2596, 2495, 2470, 2449, 2390, 2358, 2264, 2186, 1909, 1806, 1752, 1714, 1607, 1569, 1539, 1519, 1505, 1464, 1432, 1494, 1386, 1357, 1316, 1288, 1255, 1231, 1213, 1185, 1148, 1116, 1040, 998, 987, 963, 886, 858, 815, 743, 724, 690. TOF-MS calcd (found): *m/z* 233.3 (233.4) [M+]. ^{1}H NMR (500 MHz, $CDCl_3$): δ 0.91 (t, 6H, $J = 6.9$ Hz, CH_3), 1.21–1.37 [m, 8H, $(CH_2)_2$], 1.38 (sextet, 4H, $J = 7.0$, $\underline{CH_2}CH_3$), 3.35 (t, 4H, $J = 8.0$, NCH_2), 6.60 (d, 2H, $J = 7.0$ Hz, 2,6Ph), 6.62 (t, 1H, $J = 7.5$ Hz, 4Ph), 7.18 (t, 2H, $J = 7.5$ Hz, 3,5Ph).

3.1.2. N,N-dihexylaniline

74.3% yield. Product: yellow oil. FT-IR (cm^{-1}): 3986, 3647, 3412, 3093, 3061, 3024, 2958, 2873, 2735, 2649, 2596, 2495, 2470, 2449, 2390, 2358, 2264, 2186, 1909, 1806, 1752, 1714, 1607, 1569, 1539, 1519, 1505, 1464, 1432, 1494, 1386, 1357, 1316, 1288, 1255, 1231, 1213, 1185, 1148, 1116, 1040, 998, 987, 963, 886, 858, 815, 743, 724, 690. TOF-MS calcd (found): *m/z* 262.3 (262.2) [M+]. ^{1}H NMR (500 MHz, $CDCl_3$): δ 0.91 (t, 6H, $J = 6.9$ Hz, CH_3), 1.22–1.39 [m, 12H, $(CH_2)_3$], 3.35 (t, 4H, $J = 8.0$, NCH_2), 6.60 (d, 2H, $J = 7.0$ Hz, 2,6Ph), 6.62 (d, 1H, $J = 7.5$ Hz, 4Ph), 7.18 (t, 2H, $J = 7.5$ Hz, 3,5Ph).

3.2. p-N,N-dialkylaminobenzaldehydes

$POCl_3$ (22 mmol) was slowly added to anhydrous DMF (18.4 mmol) in an ice bath (−10 °C) for 30 min. To this reaction mixture *N,N*-dialkylaniline (18.4 mmol) was added, and the resulting mixture was carefully heated at 60 °C for 2 h. After hydrolysis for 2 h under vigorous stirring at r.t. using an aqueous solution of 2 N NaOH, the crude product was extracted with EtOAc. The organic layer was dried over anhydrous $MgSO_4$ and evaporated in vacuo before purification by column chromatography in silica gel (eluent: $CHCl_3$) to produce an oil. This synthetic procedure was carried out according to the Vilsmeier–Haack reaction [15]. Intermediates with different alkyl chains (propyl, butyl, pentyl and hexyl) were synthesized using the same procedure. Specific details for each compound are given below.

3.2.1. p-N,N-dipropylaminobenzaldehyde

13.2% yield. Product: colorless oil. FT-IR (cm^{-1}), 2904, 2814, 2795, 2730, 2713, 2695, 1608, 1567, 1537, 1516, 1435, 1405, 1384, 1354, 1315, 1294, 1265, 1241, 1186, 1143, 1120, 1100, 1034, 976, 816, 797, 765, 749. TOF-MS calcd (found): *m/z* 205.3 (206.2) [M+]. ^{1}H NMR (500 MHz, $CDCl_3$): δ 0.96 (t, 6H, $J = 7.5$ Hz, CH_3), 1.65 (sextet, 4H, $J = 8.0$ Hz, $\underline{CH_2}CH_3$), 3.32 (t, 4H, $J = 8.0$ Hz, NCH_2), 6.64 (d, 2H, $J = 9.0$ Hz, 3Ph), 7.70 (d, 2H, $J = 8.5$ Hz, 2Ph), 9.70 (s, 1H, CHO).

3.2.2. p-N,N-dibutylaminobenzaldehyde

10.1% yield. Product: colorless oil. FT-IR (cm^{-1}), 2904, 2814, 2795, 2730, 2713, 2695, 1609, 1570, 1540, 1518, 1434, 1403, 1388, 1356, 1314, 1286, 1263, 1223, 1186, 1147, 1122, 1107, 1017, 926, 813, 757, 727, 634. FAB-MS calcd (found): *m/z* 233.4 (233.2) [M+]. ^{1}H NMR (500 MHz, $CDCl_3$): δ 0.91 (t, 6H, $J = 7.0$ Hz, CH_3), 1.59 (sextet, 4H, $J = 7.5$ Hz, $\underline{CH_2}CH_3$), 1.66 (quintet, 4H, $J = 7.0$ Hz, $NCH_2\underline{CH_2}$), 3.20 (t, 2H, $J = 7.5$, NCH_2), 6.66 (d, 2H, $J = 9.0$ Hz, 3Ph), 7.70 (d, 2H, $J = 9.0$ Hz, 2Ph), 9.70 (s, 1H, CHO).

3.2.3. p-N,N-dipentylaminobenzaldehyde

52.0% yield. Product: colorless oil. FT-IR (cm^{-1}), 2904, 2814, 2795, 2730, 2713, 2695, 1607, 1569, 1539, 1519, 1505, 1464, 1432, 1494, 1386, 1357, 1316, 1288, 1255, 1231, 1213, 1185, 1148, 1116, 1040, 998, 987, 963, 886, 858, 815, 743, 724, 690. FAB-MS calcd (found): *m/z* 289.2 (289.2) [M+]. ^{1}H NMR (500 MHz, $CDCl_3$): δ 0.91 (t, 6H, $J = 7.0$ Hz, CH_3), 1.21–1.35 [m, 8H, $(CH_2)_2$], 1.59 (sextet, 4H,

J = 7.5 Hz, $\underline{CH_2}CH_3$), 3.20 (t, 4H, J = 7.5, NCH_2), 6.68 (d, 2H, J = 9.0 Hz, 3Ph), 7.71 (d, 2H, J = 9.0 Hz, 2Ph), 9.70 (s, 1H, CHO).

3.2.4. p-N,N-dihexylaminobenzaldehyde

12.3% yield. Product: colorless oil. FT-IR (cm^{-1}), 2904, 2814, 2795, 2730, 2713, 2695, 1607, 1569, 1539, 1519, 1505, 1464, 1432, 1494, 1386, 1357, 1316, 1288, 1255, 1231, 1213, 1185, 1148, 1116, 1040, 998, 987, 963, 886, 858, 815, 743, 724, 690. FAB-MS calcd (found): m/z 288.5 (289.2) [M+]. ^{1}H NMR (500 MHz, $CDCl_3$): δ 0.91 (t, 6H, J = 7.0 Hz, CH_3), 1.22–1.35 [m, 8H, $(CH_2)_3$], 1.59 (sextet, 4H, J = 7.5 Hz, $\underline{CH_2}CH_3$), 3.20 (t, 8H, J = 7.5, NCH_2), 6.68 (d, 2H, J = 9.0 Hz, 3Ph), 7.71 (d, 2H, J = 9.0 Hz, 2Ph), 9.70 (s, 1H, CHO).

3.3. N,N′-bis[(4-(N,N-dialkylamino)benzylidene] diaminofumaronitriles (BAR)

p-N,N-Dialkylaminobenzaldehyde (18.5 mmol) was added to a benzene solution (100 mL) containing diaminomaleonitrile (18.5 mmol) and several drops of piperidine that had been vigorously stirred for 30 min. The mixture was then refluxed by stirring for 2 h. Water was removed using a Dean-Stark trap. The reaction mixture was then cooled to room temperature. The precipitated crude product was separated by filtration and washed with cold toluene, then purified by column chromatography on silica gel using hexane/chloroform (1/1, v/v) and recrystallized from chloroform. The coupling reaction was carried out according to a previous study [16]. Products with different alkyl chains (methyl, ethyl, propyl, butyl, pentyl and hexyl) were synthesized using the same procedure. Specific details for each compound are given below.

3.3.1. N,N'-bis[(4-(N,N-dimethylamino)benzylidene] diaminofumaronitrile (BA1)

0.92% yield. Product: red-violet crystals; mp > 500 °C. FT-IR (cm^{-1}): 2967, 2929, 2899, 2869, 2204, 1281, 1729, 1688, 1611, 1571, 1525, 1482, 1432, 1411, 1392, 1367, 1336, 1317, 1266, 1230, 1183, 1147, 1116, 1059, 999, 959, 940, 806, 782, 764, 746, 726. TOF-MS calcd (found): m/z 370.4 (371.3) [M+]. ^{1}H NMR (500 MHz, $CDCl_3$): δ 3.10 (s, 12H, CH3), 6.71 (d, 4H, J = 4 Hz, 3Ph), 7.85 (d, 4H, J = 8.5 Hz, 2Ph), 8.59 (s, 2H, PhCH).

3.3.2. N,N′-bis[(4-(N,N-diethylamino)benzylidene] diaminofumaronitrile (BA2)

74.4% yield. Product: red–violet crystals; mp 278 °C. FT-IR (cm^{-1}):2967, 2929, 2899, 2869, 2204, 1607, 1561, 1513, 1436, 1410, 1377, 1349, 1316, 1266, 1195, 1139, 1118, 1036, 1076, 1010, 961, 820, 795, 727. TOF-MS calcd (found): m/z 426.6 (449.3) [Na+]. ^{1}H NMR (500 MHz, $CDCl_3$): δ 1.23 (t, 12H, J = 7.0 Hz, CH_3), 3.46 (q, 8H, J = 7.0 Hz, CH_2), 6.68 (d, 4H, J = 9.0 Hz, 3Ph), 7.82 (d, 4H, J = 8.5 Hz, 2Ph), 8.55 (s, 2H, PhCH).

3.3.3. N,N′-bis[(4-(N,N-dipropylamino)benzylidene] diaminofumaronitrile (BA3)

10.5% yield. Product: red-violet crystals; mp 213 °C. FT-IR (cm^{-1}) 2959, 2931, 2872, 2206, 1608, 1567, 1537, 1516, 1435, 1405, 1384, 1354, 1315, 1294, 1265, 1241, 1186, 1143, 1120, 1100, 1034, 976, 816, 797, 765, 749. TOF-MS calcd (found): m/z 482.7 (483.3) [M+]. ^{1}H NMR (500 MHz, $CDCl_3$): δ 0.91 (t, 12H, J = 7.0 Hz, CH_3), 1.59 (sextet, 8H, J = 7.5 Hz, $CH_3\underline{CH_2}$), 3.20 (t, 8H, J = 7.5, NCH_2), 6.68 (d, 4H, J = 9.0 Hz, 3Ph), 7.82 (d, 4H, J = 8.5 Hz, 2Ph), 8.55 (s, 2H, PhCH).

3.3.4. N,N′-bis[(4-(N,N-dibutylamino)benzylidene] diaminofumaronitrile (BA4)

34.3% yield. Product: red-violet crystals; mp 235 °C. FT-IR (cm^{-1}) 2950, 2928, 2866, 2210, 1609, 1570, 1540, 1518, 1434, 1403, 1388, 1356, 1314, 1286, 1263, 1223, 1186, 1147, 1122, 1107, 1017, 926, 813, 757, 727, 634. FAB-MS calcd (found): m/z 538.8 (539.4) [M+]. ^{1}H NMR (500 MHz, $CDCl_3$): δ 0.98 (t, 12H, J = 7.0 Hz, CH_3), 1.38 (sextet, 8H, J = 7.0 Hz, $CH_3\underline{CH_2}$), 1.63 (quintet, 8H, J = 7.0 Hz, $NCH_2\underline{CH_2}$), 3.37 (t, 8H, J = 7.0 Hz, NCH_2), 6.66 (d, 4H, J = 9.0 Hz, 3Ph), 7.81 (d, 4H, J = 9.0 Hz, 2Ph), 8.54 (s, 2H, PhCH).

3.3.5. N,N′-bis[(4-(N,N-dipentylamino)benzylidene] diaminofumaronitrile (BA5)

14.8% yield. Product: red-violet crystals; mp 209 °C. FT-IR (cm^{-1}) 2952, 2925, 2855, 2208, 1607, 1569, 1539, 1519, 1505, 1464, 1432, 1494, 1386, 1357, 1316, 1288, 1255, 1231, 1200, 1185, 1148, 1116, 1040, 998, 987, 963, 815, 743, 724, 690. FAB-MS calcd (found): m/z 594.8 (595.8) [M+]. ^{1}H NMR (500 MHz, $CDCl_3$) δ: 0.91 (t, 12H, J = 6.9 Hz, CH_3), 1.21–1.39 [m, 32H, $(CH_2)_2$], 1.59 (sextet, 8H, J = 8.0 Hz, $\underline{CH_2}CH_3$), 3.35 (t, 8H, J = 8.0, NCH_2), 6.65 (d, 4H, J = 9.5 Hz, 3Ph), 7.81 (d, 4H, J = 7.5 Hz, 2Ph), 8.54 (s, 2H, PhCH).

3.3.6. N,N′-bis[(4-(N,N-dihexylamino)benzylidene] diaminofumaronitrile (BA6)

13.5% yield. Product: red-violet crystals; mp 160 °C. FT-IR (cm^{-1}), 2952, 2925, 2855, 2208, 1607, 1569, 1539, 1519, 1505, 1464, 1432, 1494, 1386, 1357, 1316, 1288, 1255, 1231, 1200, 1185, 1148, 1116, 1040, 998, 987, 963, 815, 743, 724, 690. FAB-MS calcd (found): m/z 651.0 (651.5) [M+]. ^{1}H NMR (500 MHz, $CDCl_3$) δ: 0.91 (t, 12H, J = 6.9 Hz, CH_3), 1.25–1.38 [m, 32H, $(CH_2)_3$], 1.59 (sextet, 8H, J = 8.0 Hz, $\underline{CH_2}CH_3$), 3.35 (t, 8H, J = 8.0, NCH_2), 6.65 (d, 4H, J = 9.5 Hz, 3Ph), 7.81 (d, 4H, J = 7.5 Hz, 2Ph), 8.54 (s, 2H, PhCH).

4. Results and discussion

The UV–visible absorption and PL spectra of the analogs of BA in chloroform (8.75×10^{-6} M) are shown in Fig. 1. The absorption maxima (λ_{max}) were observed in the range of 534–550 nm with molar extinction coefficients (ε_{max}) in the range of 97,200–134,000. The absorption peaks were assigned to π–π* electronic transitions between the ground state and the excited state of the chromophore moiety [14]. The λ_{max} with large ε_{max} was suggested that an intramolecular charge- transfer chromophoric system in which the arylamine moiety was the donor and the central dicyanoethylene moiety was the acceptor. In addition, the λ_{max} gradually shifted to a longer wavelength (bathochromic shift) with an increase in the substituent a chain length, which depended on the electron donating ability of the donor moiety. PL maxima (P_{max}) of the BARs were observed in the region of 585–600 nm by excitation with the wavelength of absorption maxima. The BARs are a red-light-

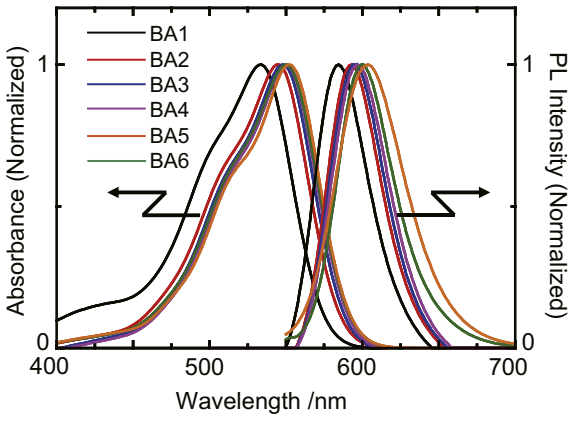

Fig. 1. Absorption spectra and PL spectra in chloroform (8.75×10^{-6} M) of BAR.

emitting materials with Stokes shifts (SS) of approximately 49 nm on average due to their symmetrical donor-accepter conjugated structures [17], although their fluorescent quantum efficiencies are very low [16,18]. In solution, the obtained photoluminescence results indicated that the alkyl substituents had no significant influence on the electronic states in the visible region.

Fig. 2 shows the absorption and PL spectra of BARs in vapor-deposited films. The absorption peaks for BAR (R = 1–6) films appeared at 588, 637, 481, 480, 491 and 485 nm, respectively. These absorption spectral changes of BAR films showed significant differences, despite their similar electronic states. Therefore, the spectral changes are correlated with the solid-state structure and are considered to depend on the alkyl chain length. A shoulder peak, which was overlapped with the absorption spectrum in solution, was assigned to the original BAR monomers. In the cases of the methyl- and ethyl-substituted BAR (BA1 and BA2) films, large bathochromic shifts were observed from the solution to the films. The intense new peaks with bathochromic shifts are a photophysical effect characteristic of J-aggregate formation, in which the interaction strength exceeds the monomeric dephasing processes [19], and indicates a head-to-tail configuration between the adjacent molecules in the films. Furthermore, the broad absorption in the short-wavelength region is assigned to the electronic transition of a short axis for the molecular conjugation length.

In contrast, the propyl-, butyl-, pentyl- and hexyl-substituted BAR (BA3, BA4, BA5 and BA6) films were found to exhibit a short-wavelength shift (hypsochromic shift). The broad spectral features with the hypsochromic shift are a photophysical effect characteristic of H-aggregate formation. The H-aggregate is formed with face-to-face stacking, with the molecules adopting a slipped-parallel structure due to the neighboring weak π–π intramolecular interaction.

Although the spectroscopic consequences of aggregation can be identified in the absorption spectra, there is also a consequence on the photoluminescence. In the case of a J-aggregate, emission occurs from the excited state, which is located at a lower energy than the corresponding monomer emission. In contrast, in the H-aggregates where the excited state is higher than the corresponding monomer excited state, there is usually a quenching of fluorescence observed in the emission spectrum of the aggregate. After excitation to the higher excited state, there is a rapid internal conversion to the lower excited state. Since the transition from the lower excited state to the ground state is not allowed, the system returns to the ground state via nonradiative decay or intersystem crossing through the triplet excited state [20]. Experimentally, the detected fluorescence shows a bathochromic shift compared to the fluorescence of the monomer. Therefore, the bathochromic shift in H-aggregates is smaller than that of J-aggregates and is not consistent with the above exiton theory.

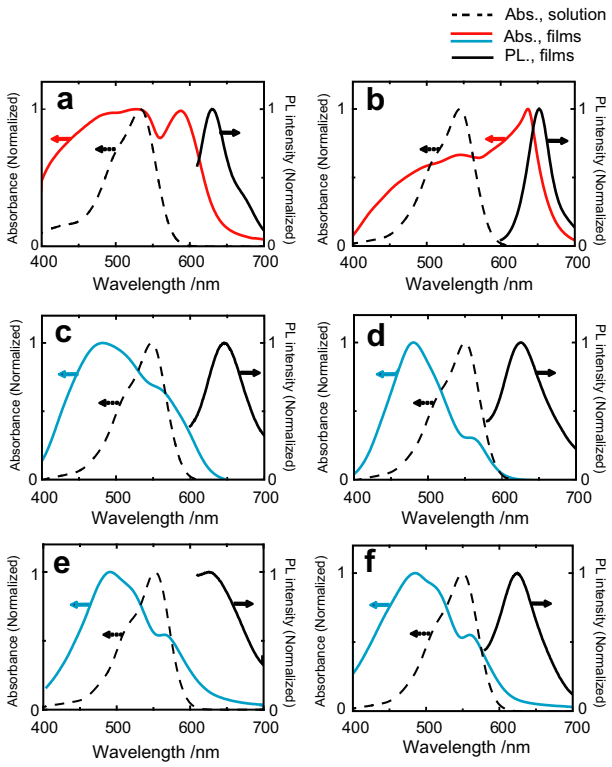

Fig. 2. Absorption spectra and PL spectra in chloroform (8.75×10^{-6} M) of (a) BA1, (b) BA2, (c) BA3, (d) BA4, (e) BA5 and (f) BA6 films.

The films of BAR analogs also showed a bright red PL laid in the wavelength region 620–650 nm by excitation with at their absorption maxima. SS between the PL peak in the film and the absorption peak in solution were 43 and 15 nm for BA1 and BA2, respectively. It is notable that the PL band is a mirror image of the low-energy edge of the J-band absorption. The small SS of the BA2 film is clearly consistent with the existence of J-aggregates. The interaction energy between monomeric transition states lowers the overall energy of the cooperative state; hence, the absorption and PL spectra of the J-aggregates show a bathochromic shift with a smaller SS relative to that in solution.

On the other hand, the absorption spectra of BA3, BA4, BA5, and BA6 films were shifted to higher energies compared with those in solution and the SS were 165, 145, 135 and 139 nm, respectively. The spectral shifts originating from H-aggregation are consistent with the results of Labarthet's study [21]. H-type molecular aggregation, an assembly in which the chromophores are arranged in such a way that their dipoles are parallel to each other, has been found mainly in Langmuir–Blodgett or self-assembled films [21–24].

All spectroscopic data of BA analogs both in solution and film are listed in Table 1. From the spectroscopic features, a remarkable difference was observed between the BA2 and BA3 films. The strong intermolecular interactions owing to the alkyl chain length account for the differences in J- and H-aggregate formation.

The surface morphologies of BAR films were examined by AFM to observe the differences between J- and H-aggregates, as shown in Fig. 3. The grain sizes in BA1, BA2, BA3, BA4 and BA5 films were found to be in the range of approximately 0.3–1.0 μm. However, the grains in the BA6 films were extremely large, with the blockish grains in the range of 2–3 μm. It is suggested that BA6 crystals grew larger since the melting point of BA6 is low, about 160 °C, compared to that of the others (BA1, 2, 3, 4 and 5: >500, 278, 213, 235, and 209 °C, respectively). From the observations, intriguingly, a significant difference could not be found in the surface morphologies of BA2 and BA3. Therefore, the details of the film structure should be investigated further.

We have summarized the results of the spectroscopic and the surface morphological features. There was no significant change in the surface morphologies between BA2 and BA3, whereas a remarkable difference was observed in BA2 and BA3 films spectroscopically. In other words, it was suggested that the critical determinant of aggregate formation of BAR is the molecular packing in thin films, which depends on the chain length of the terminal alkyl substituent. Previously, Ueda et al. reported on the aggregates of merocyanine dyes in vapor-deposited film [25]. The merocyanine dyes substituted with different alkyl chains formed either J- or H-aggregates, depending on the degree of steric hindrance between alkyl chains. These unique results were found with asymmetrical neutral molecules. A similar phenomenon has

Table 1
Substituent effects on the absorption and fluorescence spectra of BAR in solution and in films.

	$\lambda_{max}^{solution}$/nm(ε_{max}/M^{-1} cm^{-1})	$P_{max}^{solution}$/nm	$SS^{solution}$/nm[a]	λ_{max}^{film}/nm	P_{max}^{film}/nm	SS^{flim}/nm[a]	$\Delta\lambda$/nm[b]	J/H[c]
BA 1	534 (128,000)	585	51	588	631	43	54	J
BA 2	544 (140,000)	593	51	637	652	15	93	J
BA 3	548 (107,000)	594	46	481	646	165	−67	H
BA 4	550 (134,000)	598	48	480	625	145	−70	H
BA 5	552 (118,000)	603	51	491	625	134	−61	H
BA 6	550 (97,200)	600	50	485	624	139	−65	H

[a] Stokes shift (SS) = $P_{max} - \lambda_{max}$.
[b] $\Delta\lambda = \lambda_{max}^{film} - \lambda_{max}^{solution}$.
[c] J/H: J-aggregates/H-aggregates.

also been found in other molecules such as a porphyrin with a cationic surfactant [26], and a pseudoisocyanine with a polyelectrolyte [27], which formed either J- and H-aggregates.

Consequently, the BARs in this study adopted either J- and H-aggregate structures in the films despite being symmetrical and neutral molecules, and hence they have characteristics similar to the above referenced compounds. In addition, it is more important that the specific spectral properties of BAR films could be found even in an extremely thin film (ca. 50 nm). Two-dimensionally-restricted crystal growth dominated since the J- and H-aggregates could not grow with restricted film thickness. It was suggested that the slip angle in the molecular stacking is an important factor for aggregate formation. Namely, the number of the molecules was a dominant contributor to the absorption intensities in the restricted film thickness. Therefore, it was suggested that the absorption spectra of J- and H-aggregates were emphasized because the contribution of the number of molecules is much greater than that of the bulk phase within the two-dimensionally-restricted film thickness. In other words, it can be understood that crystal growth with specific spectral shifts dose not necessary correlate with defined J- and H-aggregates.

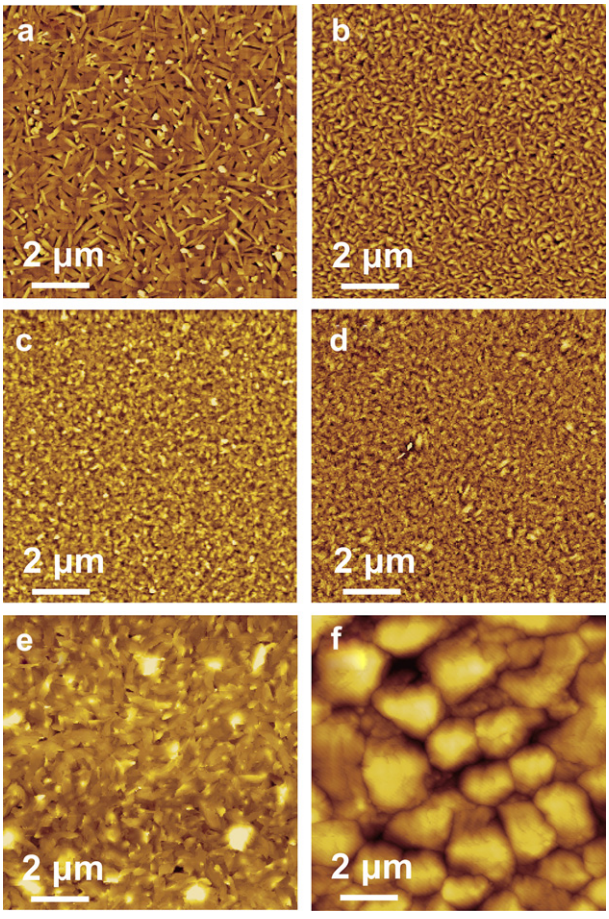

Fig. 3. AFM images (10 × 10 μm^2 surface area) of (a) BA1, (b) BA2, (c) BA3, (d) BA4, (e) BA5 and (f) BA6 films.

To summarize, in the BA1 and BA2 films, the head-to-tail intermolecular stacking structure due to the strong dipole–dipole interaction was oriented parallel to the two-dimensionally-restricted film. Judging from the spectral characteristics, J-bands which resemble typical J-aggregates, were recognized. However, in this case, it may be more appropriate to call the specific spectra "J-like bands". In the case of BA3, BA4, BA5 and BA6, the stacking plane was oriented obliquely, face-to-face, in the two-dimensionally-restricted film owing to the long alkyl chain lengths. As a result, face-to-face stacking H-aggregates as in Langmuir–Blodgett films appeared. Therefore, the J- and H-aggregates changed only due to differences in the alkyl chain length.

In the future, to confirm these conclusions, crystallographic analysis (i.e., X-ray structural analysis, electron diffraction) is necessary to understand the mechanism of J- and H-aggregate formation. Crystallographic features are more important than spectroscopic features for identification of J- and H-aggregate formation.

5. Conclusions

Bisazomethine dyes with different alkyl substituents were successfully synthesized, and their optical characteristics and surface morphologies were investigated. From this spectroscopic study, chloroform solutions of the synthesized BAR analogs exhibited similar spectral shapes and peak positions. However, in the films, BA1 and BA2 exhibited bathochromic shifts, whereas BA3, BA4, BA5 and BA6 exhibited hypsochromic shifts under the same conditions. The J- and H-aggregates in the films could be controlled by adjusting of the number of $-CH_2-$ units. Thus, it was possible to control J- and H-aggregate formation by the careful design of molecular structures. Unfortunately, the mechanism of J- and H-aggregate formation could not be identified from the spectroscopic and surface morphological studies along. Their crystallographic features will provide more information about the differences between J- and H-aggregates. This will be the subject of future studies.

References

[1] Spano FC, Siddiqui S. Exciton–vibrational coupling in pinwheel aggregates of π-conjugated molecules. Chemical Physics Letters 1999;314:481–7.
[2] Borsenberger PM, Weiss DS. Organic photoreceptors for imaging systems. New York: Marcel Dekker; 1993.
[3] Jelly EE. Spectral absorption and fluorescence of dyes in the molecular state. Nature 1936;138:1009–10.
[4] West W, Pearce S. The dimeric state of cyanine dyes. The Journal of Physical Chemistry 1965;69:1894–903.

[5] Maiti NC, Mazumdar M, Periasamy N. J- and H-aggregates of porphyrin–surfactant complexes: time-resolved fluorescence and other spectroscopic studies. The Journal of Physical Chemistry B 1998;102:1528–38.
[6] Yu J, Chen Z, Sone M, Miyata S, Li M, Watanabe T. Red-light-emitting organic electroluminescent devices with bisanil dye as emitter. Japanese Journal of Applied Physics 2001;40:3201–5.
[7] Saito K. H-aggregate formation in Squarylium Langmuir–Blodgett films. The Journal of Physical Chemistry B 2001;105:4235–8.
[8] Berlepsch HV, Bottcher C, Dahne L. Structure of J-aggregates of pseudoisocyanine dye in aqueous solution. The Journal of Physical Chemistry B 2000; 104(37):8792–9.
[9] Ikegami K, Mingotaud C, Lan M. Intramolecular charge transfer in merocyanine dye molecules enhanced by formation of J-aggregates. Thin Solid Films 2001;393:193–8.
[10] Matsumoto S, Shirai K, Kobayashi K, Wada T, Shiro M. J-aggregate structures in crystals of three bisazomethine dyes. Zeitschrift für Kristallographie 2004; 219(4):239–43.
[11] Fujieda T, Ohta K, Wakabayashi N, Higuchi S. H-aggregation of methyl orange at the interface between the water phase and oil phase in a water-in-oil microemulsion. Journal of Colloid and Interface Science 1997;185(2): 332–4.
[12] Tani K, Matsuzaki K, Kodama Y, Fukita M, Kodaira T, Horiuchi H, et al. Photophysical property of the J-aggregate thin film of an oxacyanine dye prepared by the spin-coating method and enhancement of its photostability by use of polydimethylsilane. Journal of Photochemistry and Photobiology A: Chemistry 2008;199:150–5.
[13] Matsumoto S, Kobayashi T, Aoyama T, Wada T. J-Aggregates in vapor deposited films of a bisazomethine dye. Chemical Communications 2003;15: 1910–1.
[14] Kim B-S, Kashibuchi D, Son Y-A, Kim S-H, Matsumoto S. Effect of phenyl ring substitution on J-aggregate formation ability of novel bisazomethine dyes in vapour-deposited films. Dyes and Pigments 2011;90:56–64.
[15] Raimundo JM, Blanchard P, Gallego-Planas N, Mercier N, Ledoux-Rak I, Hierle R, et al. Design and synthesis of push–pull chromophores for second-order nonlinear optics derived from rigidified thiophene-based π-conjugating spacers. The Journal of Organic Chemistry 2002;67:205–18.
[16] Kinashi K, Kotake T, Ono Y, Ishida K, Ueda Y. Photoswitching of diarylethene using bisazomethine dye. Optical Materials 2009;31(11):1711–4.
[17] Higashiguchi K, Matsuda K, Kobatake S, Yamada T, Kawai T, Irie M. Fatigue mechanism of photochromic fatigue mechanism of photochromic 1,2-Bis(2,5-dimethyl-3-thienyl)perfluorocyclopentene. Bulletin of the Chemical Society of Japan 2000;73(10):2389–94.
[18] Kim S-H, Yoon S-H, Kim S-H, Han E-M. Red electroluminescent azomethine dyes derived from diaminomaleonitrile. Dyes and Pigments 2005;64:45–8.
[19] Lemaistre JP. A two-dimensional model for energy transfer in pure and mixed J-aggregates. Chemical Physics 2007;333:186–93.
[20] Kasha M, Rawls HR, Ashraf El-Bayoumi M. The exciton model in molecular spectroscopy. Pure Appl. Chem. 1965;11:371–92.
[21] Labarthet FL, Freiberg S, Pellerin C, Pézolet M, Natansohn A, Rochon P. Spectroscopic and optical characterization of a series of azobenzene-containing side-chain liquid crystalline polymers. Macromolecules 2000;33(18):6815–23.
[22] Menzel H, Weichart B, Schmidt A, Paul S, Knoll W, Stumpe J, et al. Small-angle X-ray scattering and ultraviolet-visible spectroscopy studies on the structure and structural changes in Langmuir–Blodgett films of polyglutamates with azobenzene moieties tethered by alkyl spacers of different length. Langmuir 1994;10(6):1926–33.
[23] Ricceri R, Neto C, Abbotto A, Facchetti A, Pagani GA. Morphological characterization of H aggregates in Langmuir–Blodgett films of pyridinium–dicyanomethanide dyes. Langmuir 1999;15(6):2149–51.
[24] Moon JH, Choi JU, Kim JH, Chung H, Hahn JH, Kim SB, et al. Self-assembly of non-linear optical chromophores through ionic interactions. Journal of Materials Chemistry 1996;6(3):365–8.
[25] Ueda Y, Nitta K. Formation and characterization of aggregates of merocyanine dyes in vacuum-deposited thin film. Japanese Journal of Applied Physics 2001;40:6951–5.
[26] Koti ASR, Periasamy N. Cyanine induced aggregation in meso-tetrakis(4-sulfonatophenyl)porphyrin anions. Journal of Material Chemistry 2002; 12:2312–7.
[27] Sayama K, Tsukagoshi S, Hara K, Ohga Y, Shinpou A, Abe Y, et al. Photoelectrochemical properties of J aggregates of benzothiazole merocyanine dyes on a nanostructured TiO_2 film. The Journal of Physical Chemistry B 2002; 106(6):1363–71.